

## Dynamics of the High-Intensity Multiphoton Ionization of N<sub>2</sub>

G. N. Gibson<sup>(a)</sup> and R. R. Freeman

*AT&T Bell Laboratories, Holmdel, New Jersey 07733*

T. J. McIlrath

*Institute for Physical Science and Technology, University of Maryland, College Park, Maryland 20742*

(Received 7 May 1991)

The intensity dependence of the multiphoton photoelectron spectrum of N<sub>2</sub> has been obtained with subpicosecond laser pulses up to intensities of 10<sup>15</sup> W/cm<sup>2</sup>. Both Rydberg and valence states are observed to be ac Stark shifted into intermediate resonance during the photoionization process, although the valence states are seen only at low intensities. We show that the vibrational structure of the molecular Rydberg states cancels out in the photoelectron spectrum leading to sharp atomiclike series, even at high intensities. Photoelectrons from the ionization of each of the 3σ<sub>g</sub>, 1π<sub>u</sub>, and 2σ<sub>u</sub> electrons are clearly distinguished. We discuss implications for the interpretation of multiphoton dissociation experiments.

PACS numbers: 33.80.Rv

We present high-resolution photoelectron spectra from the multiphoton ionization (MPI) of N<sub>2</sub> up to intensities of 10<sup>15</sup> W/cm<sup>2</sup> using 308- and 616-nm laser pulses of approximately 150-fsec duration. Analysis of the spectra uses the techniques developed recently for above-threshold ionization (ATI) of rare-gas atoms in intense, subpicosecond laser fields [1]. Besides identifying the intermediate resonances in the MPI process, we can clearly distinguish the MPI of the 3σ<sub>g</sub>, 1π<sub>u</sub>, and 2σ<sub>u</sub> electrons resulting in different electronic final states. Furthermore, we show that the determination of the intensity dependence of the final-state distribution leads to a better understanding of recent experiments on the multiphoton fragmentation of N<sub>2</sub> [2]. Despite the presence of extra molecular degrees of freedom, the MPI electron spectrum of N<sub>2</sub> shows relatively simple well-resolved features attributed to intermediate Rydberg and valence-state resonances. We find that the simplification occurs for two general reasons: First, Rydberg states are only weakly coupled to the ionic core leading to a cancellation of the vibrational structure of the molecule in the electron spectrum. This results in a sharp atomiclike spectrum, even at high intensities. Second, valence states are evident only at the lowest intensities and are rapidly smeared out at high intensities by the ac Stark shift.

For atoms, the relationship between the kinetic energy of the photoelectrons in the sharp peaks obtained in high-intensity, short-pulse MPI measurements and the internal atomic structure has been extensively studied and is now well understood [3]. During the course of the laser pulse, the Rydberg levels of the atom increase their energy along with the ionization potential by an amount approximately equal to the ponderomotive potential,  $U_p = e^2 E^2 / 4m\omega^2$ , where  $E$  is the laser field at the site of the atom at any time during the pulse. If the total energy of the state becomes equal to a multiple of the photon energy, an intermediate resonance occurs in the MPI process creating a peak in the photoelectron spectrum. At high

intensities, ATI results in a series of peaks separated by the photon energy, one series for each intermediate resonance. Since the ionization potential has increased by  $U_p$ , the peaks in the series will appear at a kinetic energy of  $E_{\text{elec}} = n\hbar\omega - E_{\text{IP}} - U_p$ , where  $n\hbar\omega$  is the photon energy,  $E_{\text{IP}}$  the zero-field ionization potential, and  $n$  any integer satisfying  $E_{\text{elec}} > 0$ . The structure within each ATI series is only observed in the short-pulse regime, where the electrons experience no ponderomotive acceleration when leaving the laser focus. The electron energy can also be expressed as  $E_{\text{elec}} = m\hbar\omega - E_b$ , where  $E_b$  is the magnitude of the zero-field binding energy of the Rydberg state and  $m$  an integer.

In a molecule, there are two types of excited states, Rydberg and valence, and they behave differently in an intense laser field. A molecular Rydberg state has a large orbit and the electron is relatively decoupled from the ionic core. Different angular momentum sublevels of a Rydberg state with a given  $nl$ , built on a particular ionic core, are nearly degenerate and have the same ac Stark shift in an intense optical field. This will give rise to a sharp photoelectron peak when the state is shifted into resonance, even at high field strengths.

There is, however, a complication due to the molecular vibrational structure, which may have prevented the application of high-intensity, short-pulse photoelectron spectroscopy to molecules were it not for an important simplification. This vibrational structure would appear to produce a far more complex ATI spectrum in molecules compared to atoms, for there are many possible ionization paths for each molecular Rydberg state which is shifted into resonance. Figure 1 shows a diagram of several potential curves of N<sub>2</sub> [4], although the following discussion is perfectly general. Consider the vibrational level  $v'$  of the N<sub>2</sub><sup>+</sup>  $B$  final state and the vibrational level  $v$  of a Rydberg state built on the  $B$  state. If  $a'$  and  $a$  are vibrational constants of these states, the effective binding energy from the  $v$  to  $v'$  state will be  $E_b(v \rightarrow v') = E_b(0$

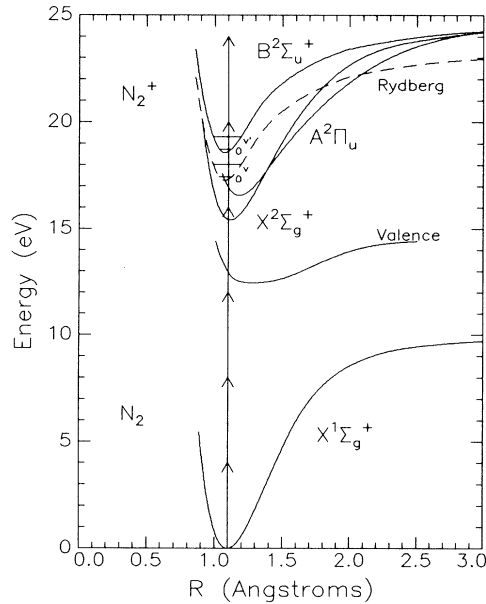


FIG. 1. Various potential curves of  $N_2$  from Ref. [4]. The arrows show the photon energy at 308 nm.

$\rightarrow 0) + a'v' - av$ . This results in  $E_{\text{elec}} = m\hbar\omega - E_b(0 \rightarrow 0) - a'v' + av$ . There are two simplifications which result in a single value for this energy: First, for Rydberg states,  $\alpha$  converges to the ionic limit  $\alpha'$  and typically differs by only a few tens of wave numbers [4], and, second, because the shape of the ionic and Rydberg potential curves are nearly identical [5], the Frank-Condon overlap integral ensures that there will be a vibrational selection rule of  $\Delta v = 0$  between the resonant and final states. The only possible electron energy is  $E_{\text{elec}} = m\hbar\omega - E_b(0 \rightarrow 0)$  independent of  $v$  and  $v'$ , exactly as in the atomic case.

In general, the higher intermediate vibrational levels of a given molecular Rydberg state come into resonance at lower intensities so, while the ac Stark shift is less, it is just compensated for by ionization to a higher vibrational energy in the final state. Thus, while all electrons resulting from a parent molecular Rydberg state have the same kinetic energy, they are ionized at different times and positions within the laser pulse and the ion is left in different vibrational final states. This result is in contrast to the analogous ionization of Rydberg states in atoms [6].

The behavior of the valence states in the strong field will be more complicated. Not only will the ac Stark shift of these states not have any simple relationship to  $U_p$ , the different total angular momentum sublevels will not shift in the laser field by the same amount, or necessarily in the same direction. Because the potential curves of the valence states and the ionic core are so different, the Frank-Condon overlap between the valence and final ionic states will not lead to the simple selection rule  $\Delta v = 0$ . The ac Stark shift of a valence state may depend on

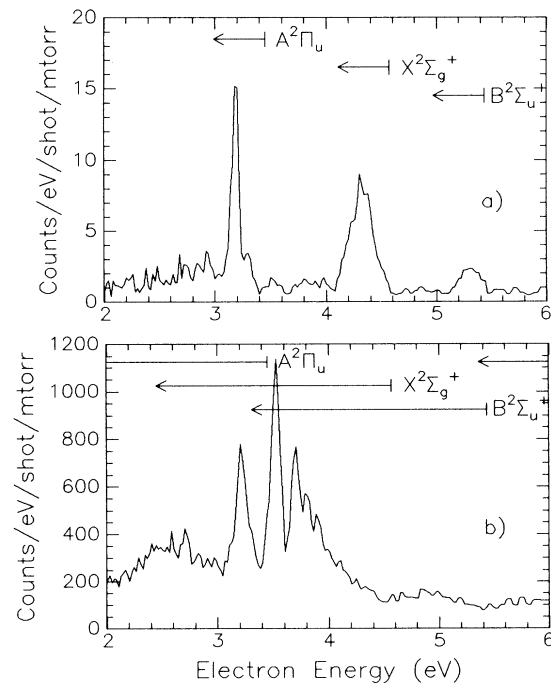


FIG. 2. Photoelectron spectra of  $N_2$  using 308-nm radiation with (a)  $23 \mu\text{J}$  and (b)  $106 \mu\text{J}$  corresponding to ponderomotive potentials of 0.46 and 2.12 eV and intensities of  $5.2 \times 10^{13}$  and  $2.4 \times 10^{14} \text{ W/cm}^2$ , respectively.

the spatial orientation of the molecules with respect to the laser field. All of these effects will lead to smearing out of valence-state resonances into the background.

The experimental apparatus and laser used in these measurements have been described elsewhere [7]. A 150-fsec, 308- or 616-nm 10-Hz laser beam with variable energy up to 1 mJ/pulse was directed into an electron energy analyzer employing a parabolic electron mirror [8]. The resolution of the analyzer is 30 meV at an electron energy of 2 eV. Spectra were binned according to laser energy in a bin width of  $\pm 10\%$  in energy. Care was taken to use sufficiently low pressure of  $N_2$  gas at all laser intensities to avoid space-charge effects [9].

Figure 2 shows electron spectra of nitrogen using the 308-nm beam at two laser energies. In nitrogen there are three different low-lying ionization potentials corresponding to the removal of the  $3\sigma_g$ ,  $1\pi_u$ , and  $2\sigma_u$  electrons (see Fig. 1), resulting in the ionic states  $X^2\Sigma_g^+$ ,  $A^2\Pi_u$ , and  $B^2\Sigma_u^+$ , respectively [4]. The value of  $n\hbar\omega - E_{\text{IP}}$  is marked in Fig. 2 by the vertical line at the base of the arrows for each of these electrons. At low intensities,  $U_p$  is small and the electrons must have energies close to  $n\hbar\omega - E_{\text{IP}}$ . Thus, the three peaks in the spectrum are the result of ionizing to the three final states  $X$ ,  $A$ , and  $B$  of the ion.

The narrow peak at 3.18 eV in Fig. 2(a) is due to the  $4f$  Rydberg state built on the  $N_2^+ A^2\Pi_u$  state [5]. The

ac Stark shift required to bring this state into resonance is  $4\hbar\omega - [E_{IP}(1\pi_u) - E_b(4f)] = 0.27$  eV, where  $E_{IP}(1\pi_u)$  is the ionization potential of the  $1\pi_u$  electron and  $E_b(4f)$  is the binding energy of the  $4f$  state. The laser energy required to produce a sufficient ponderomotive shift to just bring this state into resonance was determined experimentally to be  $13 \mu\text{J}$ . This provides an absolute calibration of the ponderomotive shift versus laser pulse energy at 308 nm for our focusing conditions:  $20 \text{ meV}/\mu\text{J}$ . (The arrows on the figures show the calculated value of the peak ponderomotive shift for the specified laser energy. Resonant features arising from a given threshold must occur within the electron energy space delineated by the arrow.)

The two other prominent peaks in Fig. 2(a) are not in the correct position to be Rydberg resonances and must be due to valence states. The greater width compared to the Rydberg resonance is expected for valence states as discussed above. Although the two peaks indicate ionization to different final states, they may be due to the same intermediate resonance. There is also no indication of a similar broad peak associated with the  $A$  state, implying that the intermediate state preferentially ionizes to the  $X$  or  $B$  state. This could be due to its electronic configuration or a preferential Frank-Condon overlap with the  $X$  and  $B$  states.

As the intensity is increased, the spectra become dominated by resonances due to Rydberg states as predicted above. At an intermediate intensity the Rydberg series based on the  $\text{N}_2^+ X^2\Sigma_g^+$  state is seen to come into resonance with four photons but the series is very weak. At the higher intensity shown in Fig. 2(b) the Rydberg series built on the  $\text{N}_2^+ B^2\Sigma_u^+$  comes into resonance with five photons, at the predicted energy of roughly  $100 \mu\text{J}$ . At the highest energy used in this experiment ( $200 \mu\text{J}$ , not shown) the  $3d$  peak of the  $B$  Rydberg series has come in at around 2.45 eV. At this intensity the  $A$  state has still not had a chance to go through the full Rydberg series of resonances and, thus, the spectrum is dominated by resonant MPI to the  $\text{N}_2^+ B^2\Sigma_u^+$  final state [10].

Electron spectra were also recorded with 616-nm radiation, shown in Fig. 3. Although this spectrum is more complex than the 308-nm data, the analysis is consistent with the above discussion. The resonances in Fig. 3 are due to Rydberg states: All of the series associated with the  $X$ ,  $A$ , and  $B$  states have gone through resonance, and the three overlapping series are identified.

The differences in the spectra taken at 616 and 308 nm are largely accounted for by the dependence of the ponderomotive potential or ac Stark shift on the wavelength ( $U_p[\text{eV}] = 9.33 \times 10^{-14} I[\text{W}/\text{cm}^2] \lambda^2[\mu\text{m}^2]$ ). Once the ponderomotive potential exceeds the photon energy, the identification of Rydberg states becomes difficult. This condition, which occurs when  $U_p \geq \hbar\omega$ , also affects the selectivity of pathways for the MPI process. For longer wavelengths many more states are shifted into resonance at relatively low intensity than for shorter wavelengths.

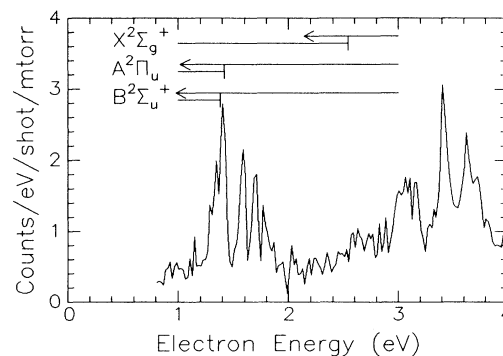
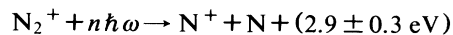


FIG. 3. Photoelectron spectrum of  $\text{N}_2$  using 616-nm radiation with  $65 \mu\text{J}$  corresponding to a ponderomotive potential of 2.4 eV and an intensity of  $6.8 \times 10^{13} \text{ W}/\text{cm}^2$ . Note that the lengths of the arrows are greater than the photon energy (2 eV) and have "wrapped" around.

At 308 nm [Fig. 2(b)], the spectrum is dominated by the  $B$  Rydberg series, which appears to be saturated. The  $X$  state has gone through resonance at much lower intensity and the full  $A$  Rydberg series has not yet come into resonance. For 616 nm (Fig. 3), all the series are seen at once. This leads to the following significant result: The  $\text{N}_2^+ B$  state will be the preferential final state for high-intensity MPI at 308 nm, while at 616 nm all the ionization channels will have a significant contribution before any one of them saturates.

This sensitivity of  $\text{N}_2$  to laser wavelength has also been noted by others in experiments analyzing the kinetic-energy distribution of the fragments following MPI and dissociation [2,11,12]. At 616 nm it is found that the ionization occurs sequentially with the fragments gaining Coulomb energy during the ionization process [12]. At 308 and 248 nm, the ionization appears to favor vertical transitions and subsequent dissociation [2,11,13]. Different photofragmentation pathways are clearly important at different wavelengths and the analysis described here indicates the role of the ponderomotive potential in determining the dominant pathways at a given laser wavelength.

As an example of the applicability of this analysis of MPI photoelectron spectroscopy to the understanding of multiphoton dissociation measurements, consider the recently reported dissociation channel of  $\text{N}_2^+$  at 305 nm [2]:



occurs when  $U_p \geq \hbar\omega$ . In these measurements the authors did not identify in which initial state the  $\text{N}_2^+$  ion originated. Our analysis shows that the  $B$  state of  $\text{N}_2^+$  is preferentially populated during MPI at 308 nm. The dissociation energy of the  $B$  state is 5.54 eV and a two-photon dissociation at 305 nm would leave a kinetic energy of  $\geq 2.6$  eV, the higher values being associated with the  $\text{N}_2^+$  ion being in an excited vibrational state. It ap-

pears likely that the dissociation reaction starts from the  $N_2^+$   $B$  state.

Photoelectron spectroscopy in the short-pulse regime reveals the role of the ponderomotive potential in the multiphoton ionization of  $N_2$  and allows a full analysis of the spectrum. The ponderomotive potential influences the resonant structure, the wavelength dependence, and the final-state distribution of the molecular ions.

This work was partially supported by AFOSR Grant No. 88-0018.

---

<sup>(a)</sup>Also at Institute for Physical Science and Technology, University of Maryland, College Park, MD 20742.

- [1] R. R. Freeman, P. H. Bucksbaum, H. Milchberg, S. Darack, D. Schumacher, and M. E. Geusic, *Phys. Rev. Lett.* **59**, 1092 (1987); P. Agostini, P. Breger, A. L'Huillier, H. G. Muller, and G. Petite, *Phys. Rev. Lett.* **63**, 2208 (1989).
- [2] C. Cornaggia, J. Lavancier, D. Normand, J. Morellec, and H. X. Liu, *Phys. Rev. A* **42**, 5464 (1990).
- [3] For a recent review, see R. R. Freeman and P. H. Bucksbaum, *J. Phys. B* **24**, 325 (1991).
- [4] A. Loftus and P. H. Krupenie, *J. Phys. Chem. Ref. Data* **6**, 113 (1977).
- [5] E. Lindholm, *Ark. Fys.* **40**, 97 (1968).
- [6] R. R. Freeman, L. D. Van Woerkom, W. E. Cooke, and T. J. McIlrath, *Laser Spectroscopy IX*, edited by M. S. Feld, J. E. Thomas, and A. Mooradian (Academic, San Diego, CA, 1989), p. 475.
- [7] P. H. Bucksbaum, L. D. Van Woerkom, R. R. Freeman, and D. W. Schumacher, *Phys. Rev. A* **41**, 4119 (1990).
- [8] D. J. Trevor, L. D. Van Woerkom, and R. R. Freeman, *Rev. Sci. Instrum.* **60**, 1051 (1989).
- [9] T. J. McIlrath, P. H. Bucksbaum, R. R. Freeman, and M. Bashkansky, *Phys. Rev. A* **35**, 4611 (1987); L. D. Van Woerkom, R. R. Freeman, W. E. Cooke, and T. J. McIlrath, *J. Mod. Opt.* **36**, 817 (1989).
- [10] The ionization of atomic nitrogen produced by some dissociative channel would result in a Rydberg spectrum nearly identical to the  $B$ -state series. However, the ion yield was measured under identical conditions and the  $N^+$  signal was less than 5% of the  $N_2^+$  signal showing that the ionization of atomic nitrogen plays a negligible role under these experimental conditions.
- [11] K. Boyer, T. S. Luk, J. C. Solem, and C. K. Rhodes, *Phys. Rev. A* **39**, 1186 (1989).
- [12] L. J. Frasinski, K. Codling, P. Hatherly, J. Barr, I. N. Ross, and W. T. Toner, *Phys. Rev. Lett.* **58**, 2424 (1987); K. Codling, L. J. Frasinski, and P. A. Hatherly, *J. Phys. B* **22**, L321 (1989).
- [13] G. Gibson, T. S. Luk, A. McPherson, K. Boyer, and C. K. Rhodes, *Phys. Rev. A* **40**, 2378 (1989).